Shortcut to stationary regimes: A simple experimental demonstration

S. Faure
Laboratoire de Collisions Agrégats Réactivité, CNRS UMR 5589, IRSAMC, Université Paul Sabatier, 118 Route de Narbonne, 31062 Toulouse CEDEX 4, France

S. Ciliberto
Université de Lyon, CNRS, Laboratoire de Physique de l'École Normale Supérieure, UMR5672, 46 Allée d'Italie, 69364 Lyon, France

E. Trizac
LPTMS, CNRS, Univ. Paris Sud, Université Paris-Saclay, 91405 Orsay, France

D. Guéry-Odelin[a)]
Laboratoire de Collisions Agrégats Réactivité, Université Paul Sabatier, 118 Route de Narbonne, 31062 Toulouse CEDEX 4, France

(Received 11 June 2018; accepted 22 November 2018)

We introduce an inverse engineering approach to drive an RC circuit. This technique is implemented experimentally (1) to reach a stationary regime associated with a sinusoidal driving voltage in a very short amount of time, (2) to ensure a fast discharge of the capacitor, and (3) to guarantee a fast change from one stationary regime to another driven at different frequencies. This work can be used as a simple experimental project dedicated to the computer control of a voltage source. Besides the specific example addressed here, the proposed method provides an original use of simple linear differential equations to control the dynamical quantities of a physical system and has therefore a certain pedagogical value.
https://doi.org/10.1119/1.5082933

I. INTRODUCTION

In most basic textbooks on electricity, the use of a time-dependent voltage source to drive a circuit is reduced to sinusoidal driving.[1] This is of paramount importance to introduce the concept of filtering in Fourier space,[2] a technique that appears in many other fields of physics[3] including wave optics.[4] Such time-dependent circuits also provide an opportunity to train the students in solving linear differential equations and give the opportunity to discuss the mechanical equivalent of an inductor, a capacitor, or a resistor.

In this article, we propose to revisit the standard RC series circuit subjected to sinusoidal driving in order to present an inverse use of the differential equation that governs the time evolution of the capacitor charge. More precisely, we show explicitly how the proper shaping of the voltage enables one to reach the stationary regime associated with sinusoidal driving in a time much shorter than the characteristic time of the circuit. Similarly, we explain how this technique can be extended to the fast discharge of a capacitor or to the sudden change in the driving frequency. Here, fast refers to a time scale small compared to the RC time constant. We detail the experimental implementation of those ideas that are well adapted to experimental classes involving computer control of an instrument, a voltage source in this case.

The method is generic and is directly inspired by the inverse engineering technique developed in the growing field of Shortcuts To Adiabaticity[5,6] with applications in classical mechanics,[7–9] optical devices,[10] quantum,[11–18] and statistical physics.[19,20]

II. DESCRIPTION OF THE SETUP

We consider a simple electric circuit made of a resistor placed in series with a capacitor[21] driven by a time dependent voltage source (see Fig. 1(a)). The charge obeys the first order differential equation

$$\dot{q}(t) + \frac{q(t)}{\tau} = \frac{V(t)}{R}, \tag{1}$$

with $\tau = RC$. For sinusoidal driving

$$V(t) = V_0 \sin(\omega t), \tag{2}$$

the solution of Eq. (1) is given by the superposition of the response with the source V set to zero and the forced response: $q(t) = q_0(t) + q_f(t)$. In mathematical language, we call these two responses the homogeneous and the particular solutions. The homogeneous solution reads $q_0(t) = A_0 \exp(-t/\tau)$, while the particular inhomogeneous solution is of the following form:

$$q_f(t) = A_1^\omega \sin(\omega t) + A_2^\omega \cos(\omega t). \tag{3}$$

We readily find $A_1^\omega = (V_0\tau/R)/(1+\omega^2\tau^2)$ and $A_2^\omega = -\omega\tau A_1$. Using the amplitude phase notation $q_f(t) = A\sin(\omega t - \varphi)$ with $\varphi = \arctan(\omega\tau)$ and $A = (V_0\tau/R)/\sqrt{1+\omega^2\tau^2}$. With this notation, we clearly see the existence of a time delay, φ/ω, between the driving and the response obtained through the time evolution of the charge. It is worth noting that the forced solution is a particular solution of the second order differential equation without dissipation

$$\ddot{q}_f + \omega^2 q_f = 0. \tag{4}$$

The constant A_0 is determined by the initial condition on the full solution. Assuming that the charge is zero initially, $q(0) = 0$, we find

$$q(t) = \frac{V_0\tau/R}{1+\omega^2\tau^2}\left\{\sin(\omega t) - \omega\tau\left[\cos(\omega t) - e^{-t/\tau}\right]\right\}. \tag{5}$$

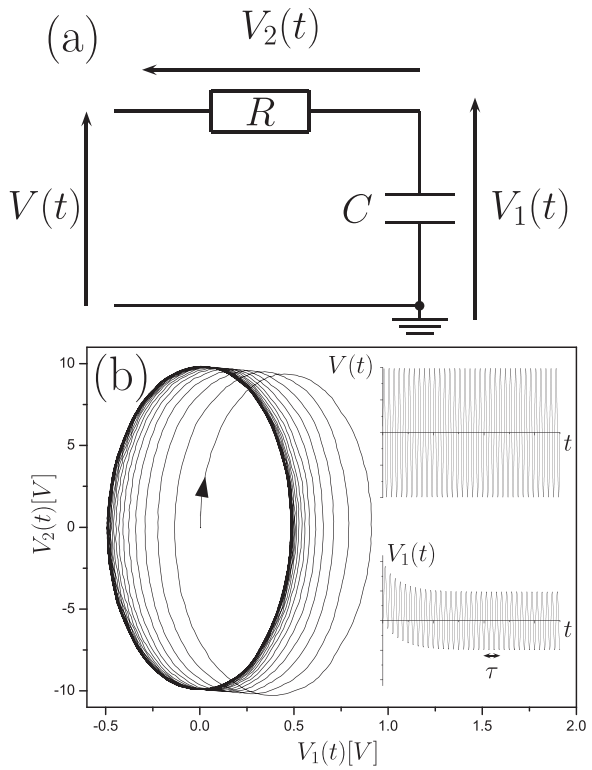

Fig. 1. (a) The RC circuit under study. (b) Phase portrait of our system, displaying the measured evolution of the voltage $V_2(t) = \tau \dot{V}_1(t)$ as a function of $V_1(t)$ for a voltage source $V(t) = V_0 \sin(\omega t)$. Here, $V_0 = 10\,\mathrm{V}$, $\omega/2\pi = 10\,\mathrm{kHz}$, $\tau = 327.5\,\mu\mathrm{s}$, and 10 000 experimental data points have been gathered to produce the curve, with a subsequent average over 20 realizations. The insets provide the explicit variation with time of the voltage source, $V(t)$, and the voltage drop across the capacitor, $V_1(t)$.

The transient regime lasts over the time interval for which the term $e^{-t/\tau}$ is not negligible with respect to one. The time t_∞ required to reach the stationary regime should be such that[22] $\omega\tau e^{-t_\infty/\tau} \ll 1$. In the limit $\omega\tau \gg 1$, the charge and therefore the current undergo a large number of oscillations before reaching the stationary regime. This transient towards the stationary regime is most conveniently observed in the so-called phase space $(q, \dot{q})$:[23] the system converges towards an elliptical attractor[24] whose size is dictated by the driving voltage amplitude and the characteristics of the circuit

$$\left(q^2(t) + \frac{1}{\omega^2}\left(\frac{dq}{dt}\right)^2\right) \underset{t \gg \tau}{\rightarrow} \frac{(V_0\tau/R)^2}{1+\omega^2\tau^2}. \tag{6}$$

In Fig. 1(b), we have constructed such a phase space representation by plotting the voltage $V_2(t)$ (proportional to dq/dt) as a function of $V_1(t)$ (proportional to $q(t)$) for the following experimental parameters: $V_0 = 10\,\mathrm{V}$, $R = 9.9863 \times 10^3 \pm 1.1\ \Omega$, $C = 32.8 \pm 0.49$ nF (measured with a multimeter Agilent 34405A), $\tau = RC = 327.5\,\mu\mathrm{s}$, $\omega = 2\pi \times 10\ 000\,\mathrm{Hz}$, and an acquisition time of $35 \times 2\pi/\omega$.

The dimensionless parameter $\omega\tau = 20.5$ has been chosen sufficiently large to ensure that the system undergoes a significant number of oscillations before reaching the stationary regime. The voltage $V_1(t)$ has been recorded using a LeCroy Wavesurfer44Xs oscilloscope (10 000 data points are acquired) and averaged over 20 repetitions of the protocol. The voltage $V_2(t)$ cannot be obtained directly since both the voltage source and the oscilloscope that reads the $V_1(t)$ voltage are connected to ground. We therefore inferred the voltage $V_2(t)$ by numerically performing the subtraction: $V_2(t) = V(t) - V_1(t)$. We observe on the phase plot the well-known clockwise rotation of the trajectory together with the limit cycle (visible as the thick ellipse), which sets in after a long time.

III. OUR APPROACH

In the following, we propose to engineer the voltage source to reach the stationary regime on a much shorter time scale $t_f \ll \tau$. For $t > t_f$, the voltage will be the sinusoidal driving voltage given by (2). Within our approach, t_f can be chosen at will, in principle, arbitrarily small.[25] We adopt an inverse engineering approach. To this end, we first fix the boundary conditions that we would like on the charge $q(t)$: $q(0) = 0$, and $q(t_f) = q_f(t_f)$, $\dot{q}(t_f) = \dot{q}_f(t_f)$ and $\ddot{q}(t_f) = \ddot{q}_f(t_f) = -\omega^2 q_f(t_f)$. The last condition is important since the stationary trajectory we aim to reach is a solution of the second-order linear differential equation (4). We add the two following constraints $\dot{q}(0) = 0$ and $\ddot{q}(0) = 0$ to ensure a smooth initial variation of the charge. As the motion of the charge is sinusoidal, the boundary conditions on the first and second derivatives must be chosen consistently. The second step consists in choosing an interpolation function for the charge. Having set 6 boundary conditions, we will therefore use an interpolation function featuring 6 free parameters. In practice and for the sake of simplicity, we take a fifth order polynomial

$$\begin{aligned} q(t) = &\left[10q(t_f) - 4t_f\dot{q}(t_f) + t_f^2\ddot{q}(t_f)/2\right]\left(\frac{t}{t_f}\right)^3 \\ &+\left[-15q(t_f) + 7t_f\dot{q}(t_f) - t_f^2\ddot{q}(t_f)\right]\left(\frac{t}{t_f}\right)^4 \\ &+\left[6q(t_f) - 3t_f\dot{q}(t_f) + t_f^2\ddot{q}(t_f)/2\right]\left(\frac{t}{t_f}\right)^5. \end{aligned} \tag{7}$$

By plugging this time-dependent form for the charge into Eq. (1), we find the voltage $V(t)$ that we should impose on the circuit to obtain the desired evolution of the charge. This is the essence of the inverse engineering technique.

As a concrete example, we propose to reach the stationary regime in a quarter of the driving period $t_f = \pi/(2\omega)$ (see Fig. 2(a)). As a result, we fix the final values for the charge $q(t_f) = A_1^\omega$, $\dot{q}(t_f) = -\omega A_2^\omega$, $\ddot{q}(t_f) = -\omega^2 q(t_f)$. With such boundary conditions, we have found the following voltage for the time interval $0 \le t \le t_f$:

$$\begin{aligned} V(t) = -\frac{V_0}{2}\left(\frac{t}{t_f}\right)^2 \frac{1}{1+\omega^2\tau^2}\Bigg\{a_2 + a_3\left(\frac{t}{t_f}\right) \\ +a_4\left(\frac{t}{t_f}\right)^2 + a_5\left(\frac{t}{t_f}\right)^3\Bigg\}, \end{aligned} \tag{8}$$

with

$$\begin{aligned} a_2 &= 3\left(\frac{\tau}{t_f}\right)\left[-20 + 8\omega^2\tau t_f + (\omega t_f)^2\right], \\ a_3 &= 120\frac{\tau}{t_f} + (\omega t_f)^2 - 4\Big(5 + 14(\omega\tau)^2\Big), \\ a_4 &= -60\frac{\tau}{t_f} - 2(\omega t_f)^2 - 9\omega^2\tau t_f + 30\Big(1 + (\omega\tau)^2\Big), \\ a_5 &= -12 + 6\omega^2\tau t_f + (\omega\tau)^2. \end{aligned} \tag{9}$$

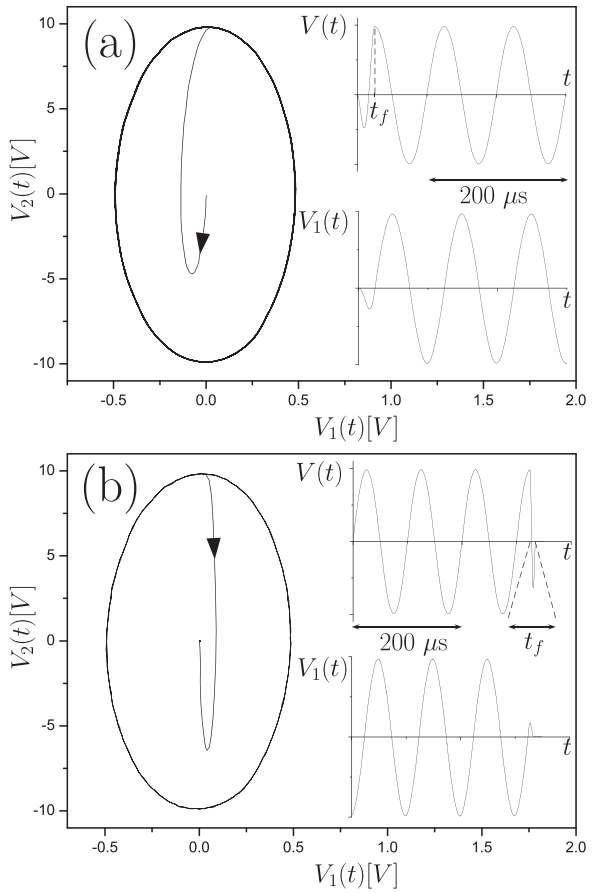

Fig. 2. (a) Experimental evolution of the voltage $V_2(t) = \tau \dot{V}_1(t)$ as a function of $V_1(t)$ for a shaped voltage $V(t)$ imposed to the RC circuit. Here, the target time t_f is chosen to be $t_f = \pi/(2\omega) = 25\,\mu$s. From t equal to zero to $\pi/(2\omega)$, the signal $V(t)$ has been calculated to force the evolution of the charge towards the stationary regime and to be continuously connected to the sinusoidal driving voltage for $t \geq t_f$. (b) Experimental evolution of the voltage $V_2(t)$ as a function of $V_1(t)$ for the driving voltage that ensures the discharge of the capacitor in $t_f = 10\,\mu$s for an initial charge in the stationary regime associated with the driving frequency 10 kHz. The amplitude and frequency are the same as for Fig. 1. Insets represent the voltages $V(t)$ and $V_1(t)$ as a function of time.

These coefficients satisfy all our boundary conditions. For $t \geq t_f$, the voltage is simply the sinusoidal driving voltage (see Eq. (2)). To drive the voltage source, $V(t)$, with such a time dependency, we use the LabVIEW control of the arbitrary waveform generator Keysight 33611A (see upper insets of Fig. 2(a)). The imposed source voltage is discretized with a time step of 2.5 ns. Interestingly, our fast protocol for the chosen boundary values does not exhibit a voltage overshoot: the designed voltage has an amplitude always smaller than or equal to $V_0 = 10$ V in our experiment. The resulting measured voltages are summarized in the phase space plot of Fig. 2(a). As expected, we observe the rapid convergence towards the stationary regime. Comparing the inset of Fig. 2(a), one clearly observes that the charge time evolution measured through $V_1(t)$ responds to the change in the voltage source $V(t)$ with a delay. It is worth noticing that the convergence towards the stationary regime has been dramatically accelerated thanks to our protocol as it can be seen by comparing Figs. 1(b) and 2(a). The stationary regime is approximately reached in a time $6\tau \simeq 2$ ms when the voltage source is applied suddenly while our fast protocol requires a quarter of a period $\pi/2\omega = 25\,\mu$s. The gain in time is therefore about 2 orders of magnitude. We have taken boundary conditions at a final time for a quarter of period just for convenience and simplicity, but the method still holds for shorter amounts of time.

In a similar manner, the reverse transformation from the stationary regime to the complete discharge of the capacitor can also be driven in a short amount of time. The calculation of the desired voltage is obtained in the very same manner using the proper boundary conditions for the charge. Figure 2(b) (lower panel) illustrates such an experimental realization with the same electrical circuit using $V_0 = 10$ V, $\omega/2\pi = 10$ kHz, and $t_f = 10\,\mu$s.

Combining the previous methods, one can readily extend the control of the circuit driving to connect two stationary states associated with two different driving frequencies, going through the state of "rest" (vanishing V_1 and V_2) as an intermediate. We have realized this experiment by driving the system at 20 kHz and then at 10 kHz as explicitly shown in Fig. 3. We present in the upper panel such a transformation performed with a sudden change in the frequency and in the lower panel the reaching of the new stationary regime in $t_f = 35\,\mu$s thanks to a proper shaping of the voltage source (see the inset of Fig. 3(b)).

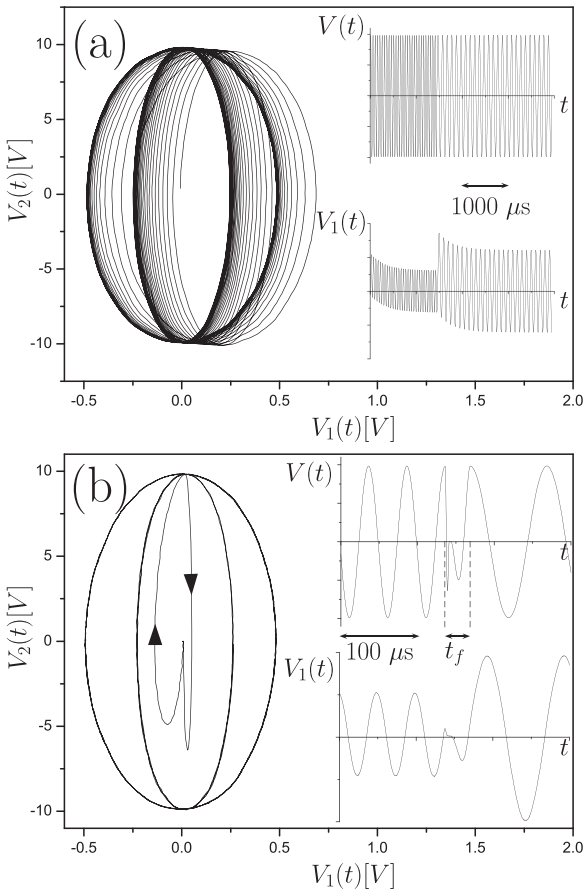

Fig. 3. (a) Phase portrait representation ($V_2(t)$ as a function of $V_1(t)$). The circuit undergoes a sudden frequency change from a sinusoidal driving frequency at 20 kHz to 10 kHz. We observe the convergence towards the initial stationary state (internal ellipse) to the targeted one (external ellipse). (b) Similar plot using the inverse engineering technique to accelerate the change in the stationary regime and operate the switch in a chosen time t_f. The voltage is engineered in a non-sinusoidal manner during a time span $t_f = 10 + 25 = 35\,\mu$s to ensure first the passage from the stationary regime at 20 kHz to a complete discharge and then from $q = 0$ to the stationary regime associated with the frequency 10 kHz. Same notation as in Fig. 2 for the insets.

IV. CONCLUSION

In conclusion, we have shown both theoretically and experimentally the usefulness of inverse engineering to drive at will the current in a RC circuit. Our treatment offers specific projects and activities for students that feature both conceptual/mathematical and experimental aspects. While the most rewarding option is to treat both questions in class, it is also possible to restrict to a one-sided treatment. For a successful implementation, we have provided after Eq. (6) a relevant set of parameter values. The idea can be easily implemented as a computer-interfacing project. From a pedagogical point of view, such studies also contribute to the renewal of the teaching of differential equations with application in the growing field of control in physics. This method can be readily generalized to other linear circuits such as the RLC circuit. Using the analogy between electricity and classical mechanics, the technique provides interesting and nontrivial solutions in this latter domain. For instance, the transport of a particle in a moving harmonic trap obeys the second-order linear differential equation as follows:

$$\ddot{x} + \omega_0^2 x = \omega_0^2 x_0^2, \tag{10}$$

where x denotes the position of the particle and x_0 that of the bottom (i.e., the center) of the potential. An optimal transport over a distance d of a particle initially at rest and that reaches its final position at rest imposes the following boundary conditions: $x(0) = 0$, $\dot{x}(0) = 0$, $\ddot{x}(0) = 0$, $x(t_f) = d$, $\dot{x}(t_f) = 0$, and $\ddot{x}(t_f) = 0$, with $x_0(0) = 0$ and $x_0(t_f) = d$. The position $x(t)$ is chosen by interpolation between the initial and final boundary conditions, and the instantaneous position of the trap, $x_0(t)$, is then inferred from Eq. (10). The method can be further improved to take into account non-harmonic traps[9] or to guarantee robust transport.[8] Similarly, this idea has been used to drive, at will, a spin or two spins to generate entangled states.[26]

As presented here, inverse engineering is quite simple and does not require a sophisticated mathematical formalism. It is worth emphasizing that it differs from optimal control theory, which aims at extremalizing a given objective (or cost) function,[27] under some constraints.[28,29] Here, the protocols we advocate are not meant to be optimal but to perform a given task in a specific, and short, time span.

Other general methods to speed up quantum transformations have been put forward in the context of quantum mechanics such as the counterdiabatic method,[30,31] the Lewis-Riesenfeld invariant methods,[32,33] the fast-forward method,[35] or techniques relying on the Lie algebra.[34] Some of those techniques have been recently transposed in the classical world[6,7] not only in mechanics but also in statistical physics.[20,36,37]

ACKNOWLEDGMENTS

It is a pleasure to thank J. Vigué and P. Cafarelli for fruitful discussions. This work was supported by Programme Investissements d'Avenir under Program No. ANR-11-IDEX-0002-02, Reference No. ANR-10-LABX-0037-NEXT, and the LabEx PALM program (No. ANR-10-LABX-0039-PALM) and the research funding Grant No. ANR-18-CE30-0013 from the Agence Nationale de la Recherche.

[a]Electronic mail: dgo@irsamc.ups-tlse.fr

[1]E. M. Purcell and D. J. Morin, *Electricity and Magnetism*, 3rd ed. (Cambridge U. P., New York, 2012).
[2]P. Cafarelli, J.-P. Champeaux, M. Sence, and N. Roy, "The RLC system: An invaluable test bench for students," Am. J. Phys. **80**, 789–799 (2012).
[3]M. Sabieh Anwara, J. Alam, M. Wasif, R. Ullah, S. Shamim, and W. Zia, "Fourier analysis of thermal diffusive waves," Am. J. Phys. **82**, 928–933 (2014).
[4]J. E. Rhodes, Jr., "Analysis and synthesis of optical images," Am. J. Phys. **21**, 337–338 (1953).
[5]E. Torrontegui *et al.*, "Shortcuts to adiabaticity," Adv. At. Mol. Opt. Phys. **62**, 117–169 (2013).
[6]S. Deffner, C. Jarzynski, and A. del Campo, "Classical and quantum shortcuts to adiabaticity for scale-invariant driving," Phys. Rev. X **4**, 021013 (2014).
[7]C. Jarzynski, "Generating shortcuts to adiabaticity in quantum and classical dynamics," Phys. Rev. A **88**, 040101(R) (2013).
[8]D. Guéry-Odelin and J. G. Muga, "Transport in a harmonic trap: Shortcuts to adiabaticity and robust protocols," Phys. Rev. A **90**, 063425 (2014).
[9]Q. Zhang, X. Chen, and D. Guéry-Odelin, "Fast and optimal transport of atoms with non-harmonic traps," Phys. Rev. A **92**, 043410 (2015).
[10]Tzung-Yi Lin, Fu-Chen Hsiao, Yao-Wun Jhang, Chieh Hu, and Shuo-Yen Tseng, "Mode conversion using optical analogy of shortcut to adiabatic passage in engineered multimode waveguides," Opt. Express **20**, 24085–24092 (2012).
[11]A. Couvert, T. Kawalec, G. Reinaudi, and D. Guéry-Odelin, "Optimal transport of ultracold atoms in the non-adiabatic regime," Europhys. Lett. **83**, 13001 (2008).
[12]J.-F. Schaff, X. L. Song, P. Capuzzi, P. Vignolo, and G. Labeyrie, "Shortcut to adiabaticity for an interacting Bose-Einstein condensate," Europhys. Lett. **93**, 23001 (2011).
[13]A. Walther, F. Ziesel, T. Ruster, S. T. Dawkins, K. Ott, M. Hettrich, K. Singer, F. Schmidt-Kaler, and U. Poschinger, "Controlling fast transport of cold trapped ions," Phys. Rev. Lett. **109**, 080501 (2012).
[14]R. Bowler, J. Gaebler, Y. Lin, T. R. Tan, D. Hanneke, J. D. Jost, J. Home, D. Leibfried, and D. J. Wineland, "Coherent diabatic ion transport and separation in a multizone trap array," Phys. Rev. Lett. **109**, 080502 (2012).
[15]M. G. Bason, M. Viteau, N. Malossi, P. Huillery, E. Arimondo, D. Ciampini, R. Fazio, V. Giovannetti, R. Mannella, and O. Morsch, "High-fidelity quantum driving," Nat. Phys. **8**, 147–152 (2012).
[16]W. Rohringer, D. Fischer, F. Steiner, I. Mazets, J. Schmiedmayer, and M. Trupke, "Non-equilibrium scale invariance and shortcuts to adiabaticity in a one-dimensional Bose gas," Sci. Rep. **5**, 9820 (2015).
[17]Y.-X. Du, Z.-T. Liang, Y.-C. Li, X.-X. Yue, Q.-X. Lv, W. Huang, X. Chen, H. Yan, and S.-L. Zhu, "Experimental realization of stimulated Raman shortcut-to-adiabatic passage with cold atoms," Nat. Commun. **7**, 12479 (2016).
[18]B. B. Zhou, A. Baksic, H. Ribeiro, C. G. Yale, F. J. Heremans, P. C. Jerger, A. Auer, G. Burkard, A. A. Clerk, and D. D. Awschalom, "Accelerated quantum control using superadiabatic dynamics in a solid-state lambda system," Nat. Phys. **13**, 330 (2017).
[19]D. Guéry-Odelin, J. G. Muga, M. J. Ruiz-Montero, and E. Trizac, "Exact non-equilibrium solutions of the Boltzmann equation under a time-dependent external force," Phys. Rev. Lett. **112**, 180602 (2014).
[20]I. A. Martinez, A. Petrosyan, D. Guéry-Odelin, E. Trizac, and S. Ciliberto, "Engineered swift equilibration of a Brownian particle," Nat. Phys. **12**, 843 (2016).
[21]T. J. Kelly, "Advanced undergraduate RC circuits: An experimentalist's perspective," Eur. J. Phys. **36**, 055041 (2015).
[22]For our parameters, $\omega\tau \sim 20.6$, so we can take $t_\infty > 6\tau$ which guarantees that $\omega\tau e^{-t_\infty/\tau} < 0.05$.
[23]A. Deprit, "Free rotation of a rigid body studied in the phase plane," Am. J. Phys. **35**, 424–428 (1967).
[24]The attractor in phase space is defined as the parametric representation in the $(q, \dot{q})$ space of the forced solution, i.e., solution (5) without the decaying exponential term. It is thus the locus of points $(q(t), \dot{q}(t))$, parametrized by time t, which yields an ellipse.
[25]In practice, the voltage step provides a limitation for t_f, so the simple capacitor-resistor model that we are using here is valid for times larger than the circuit size over the speed of light (say 1 ns). Below this time scale, wave-like effects will play a role and a more elaborate circuit model is required.
[26]Qi Zhang, Xi Chen, and D. Guéry-Odelin, "Reverse engineering protocols for controlling spin dynamics," Sci. Rep. **7**, 15814 (2017).
[27]D. Anderson, F. Andersson, P. Andersson, A. Billander, M. Desaix, and M. Lisak, "The optimal journey from A to B," Am. J. Phys. **76**, 863–866 (2008).

[28]M. Athans and P. L. Falb, *Optimal Control. An Introduction to the Theory and Its Applications* (McGraw-Hill Book Co., New York, 1966).
[29]K. Altmann, S. Stingelin, and F. Tröltzsch, "On some optimal control problems for electrical circuits," Int. J. Circuit Theory Appl. **42**, 808–866 (2014).
[30]M. Demirplak and S. A. Rice, "Adiabatic population transfer with control fields," J. Phys. Chem., A **107**, 9937–9945 (2003).
[31]M. V. Berry, "Transitionless quantum driving," J. Phys., A **42**, 365303 (2009).
[32]Xi Chen, A. Ruschhaupt, S. Schmidt, A. del Campo, D. Guéry-Odelin, and J. G. Muga, "Fast optimal frictionless atom cooling in harmonic traps: Shortcut to adiabaticity," Phys. Rev. Lett. **104**, 063002 (2010).
[33]X. Chen, E. Torrontegui, and J. G. Muga, "Lewis-Riesenfeld invariants and transitionless quantum driving," Phys. Rev. A **83**, 062116 (2011).
[34]E. Torrontegui, S. Martinez-Garaot, and J. G. Muga, "Hamiltonian engineering via invariants and dynamical algebra," Phys. Rev. A **89**, 043408 (2014).
[35]S. Masuda and K. Nakamura, "Fast-forward problem in quantum mechanics," Phys. Rev. A **78**, 062108 (2008).
[36]J. Deng, Q.-H. Wang, Z. Liu, P. Hänggi, and J. Gong, "Boosting work characteristics and overall heat-engine performance via shortcuts to adiabaticity: Quantum and classical systems," Phys. Rev. E **88**, 062122 (2013).
[37]G. Li, H. T. Quan, and Z. C. Tu, "Shortcuts to isothermality and nonequilibrium work relations," Phys. Rev. E **96**, 012144 (2017).

Keuffel and Esser Mechanical Drawing Instruments

In the summer of 1964 I sat down to draw the figures for my doctoral thesis. I used a set of mechanical drawing instruments very much like the rather complete set in the picture. The instruments were made by Keuffel and Esser, a firm founded by a pair of German immigrants in 1867. The offices were in lower Manhattan, and the instruments were made in their factory in Hoboken across the Hudson River. The company also manufactured slide rules, including the Thacher calculating device in an earlier segment of this series. The drawing pens were a devil to use, as they had two parallel blades with pointed ends that were adjusted to *almost* touch each other, and a droplet of ink was held between the blades. The slightest shake of the hand dropped a blot of ink on the paper, ruining the diagram. This set came to the Greenslade Collection from the Kenyon College mathematics department. (Picture and text by Thomas B. Greenslade, Jr., Kenyon College)